

**ICSV14**  
Cairns • Australia  
9-12 July, 2007



## **AN ANALYSIS OF THE CHANGES TO THE MECHANICAL AND ACOUSTICAL PROPERTIES OF PAPER CAUSED BY THE DAMAGE MECHANISMS PRESENT IN THE FIBRE STRUCTURE**

David Kao<sup>1</sup>, Deryn Graham<sup>1</sup> and Koulis Pericleous<sup>1</sup>

<sup>1</sup>School of Computing and Mathematical Sciences, University of Greenwich, Park Row, Greenwich, London, SE10 9LS  
[d.kao@gre.ac.uk](mailto:d.kao@gre.ac.uk)

### **Abstract**

This paper will analyse two of the likely damage mechanisms present in a paper fibre matrix when placed under controlled stress conditions: fibre/fibre bond failure and fibre failure. The failure process associated with each damage mechanism will be presented in detail focusing on the change in mechanical and acoustic properties of the surrounding fibre structure before and after failure. To represent this complex process mathematically, geometrically simple fibre arrangements will be chosen based on certain assumptions regarding the structure and strength of paper, to model the damage mechanisms. The fibre structures are then formulated in terms of a hybrid vibro-acoustic model based on a coupled mass/spring system and the pressure wave equation. The model will be presented in detail in the paper. The simulation of the simple fibre structures serves two purposes; it highlights the physical and acoustic difference of each damage mechanism before and after failure, and also shows the differences in the two damage mechanisms when compared with one another.

The results of the simulations are given in the form of pressure wave contours, time-frequency graphs and Continuous Wavelet Transform (CWT) diagrams. The analysis of the results leads to criteria by which the two damage mechanisms can be identified. Using these criteria it was possible to verify the results of the simulations against experimental acoustic data. The models developed in this study are of specific practical interest in the paper-making industry, where acoustic sensors may be used to monitor continuous paper production. The same techniques may be adopted more generally to correlate acoustic signals to damage mechanisms in other fibre-based structures.

### **1. INTRODUCTION**

This paper will present a detailed analysis of the two proposed damage mechanisms, namely the fibre/fibre bond failure and the fibre failure, present in a paper fibre matrix when placed under controlled stress conditions. The failure process for each damage mechanism will be examined in detail, with the analysis focussing on the change in the mechanical and acoustical properties of the fibre structure caused by the fibre damage.

The fibre structures are simulated using a hybrid vibro-acoustic model developed by Kao *et al.* [1, 2], by coupling together two well known systems, the mass/spring paradigm [3, 4] and the acoustic wave equation [5,6]. The model will be used to simulate the acoustic response of several simple fibre structures using various interpretive techniques including the Continuous Wavelet Transform (CWT) [7, 8, 9], to ascertain the change in the mechanical and acoustic properties of the fibre structures undergoing the different failure types. The CWT provides critical temporal information on the different frequency components of the acoustic emission (AE), which establishes suitable criteria for the identification of the two damage mechanisms. The software to calculate the CWT is provided by Vallen-Systeme [10].

## 2. THE VIBRO-ACOUSTIC MODEL

The vibro-acoustic approach employs the mass/spring model to simulate the movement of the fibre structure as shown by Equation (1).

$$m_i \frac{d^2 \mathbf{r}_i}{dt^2} + \sum_j k_{ij} (||\mathbf{r}_j - \mathbf{r}_i|| - L_{i,j}) \frac{\mathbf{r}_j - \mathbf{r}_i}{||\mathbf{r}_j - \mathbf{r}_i||} + b_i \frac{d\mathbf{r}_i}{dt} = 0 \quad (1)$$

where  $\mathbf{r}$  is the mass position vector,  $m_i$  is the mass of mass  $i$ ,  $b_i$  is the damping constant on mass  $i$  and  $k_{ij}$  is the stiffness and  $L_{ij}$  is the original length of the spring connecting masses  $i$  and  $j$ .

The movement from the mass/spring model is coupled to the acoustic pressure wave equation shown in Equation (2), by means of Equation (3).

$$\frac{\partial^2 p}{\partial t^2} = c^2 \left( \nabla^2 p - \nabla \cdot \mathbf{F} + \rho \frac{\partial q}{\partial t} \right) \quad (2)$$

$$\frac{\partial q}{\partial t} = \frac{d\mathbf{u}_{ms}}{dt} \quad (3)$$

where  $p$  is the acoustic pressure,  $c$  is the speed of sound in the medium,  $\mathbf{F}$  is an external force,  $\rho \frac{\partial q}{\partial t}$  is known as the volumetric acceleration and  $\mathbf{u}_{ms}$  is the velocity vector of the masses from the mass/spring model. For a discussion on the numerical implementation of the vibro-acoustic model refer to Kao *et al.*[2]. The numerical model can now be used to simulate the damage mechanisms in paper using several simple fibre structures. However, it is necessary to first discuss the assumptions associated with the paper fibre structure.

## 3. ASSUMPTIONS OF THE PAPER FIBRE STRUCTURE

To successfully model the acoustic response of the two damage mechanisms, several assumptions regarding the fibre structure and individual fibre properties must be properly addressed.

### 3.1 Free Vibrating Length

Figure 1 shows a typical notched paper sample stressed at 98% of its failure load. The two opaque regions located next to each notch show the area of the paper that has already

undergone significant damage. More importantly, it shows that the length of the damage zone is no more than 1 mm in length. Therefore it is assumed that the fibre structure outside of the damage zone remains in its virgin state. If no deformation has occurred then the fibre structure outside of the damage zone can be thought of as having an infinite mass. This leads to the first assumption that the free vibrating length of a paper fibre in the damage zone is equal to 1 mm.

### 3.2 Extension of the Paper Fibre

Figure 2 shows the extension of the paper specimen versus the AE number. The paper sample has a length of 100 mm and undergoes a maximum extension of 0.85 mm. This equates to approximately 1% of the length of the paper sample. For simplicity, it is assumed that the internal structure of the paper is a Cartesian mesh of fibres so that an extension of 1% in the macroscopic length of the paper translates to an extension of 1% in each fibre.

### 3.3 Material Properties of the Paper Fibre

The previous two sections have dealt with the variables  $L$  and  $x$  in Equation (5). The remainder of the material properties are average values as stated by Gregerson [11].

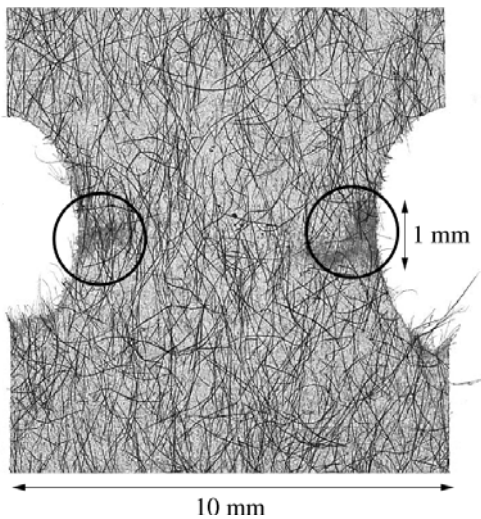


Figure 1 – Sample Showing the Size of the Damage Zone in the Paper

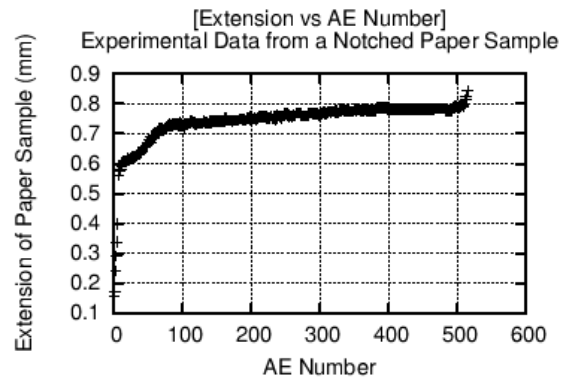


Figure 2 – Extension of a Typical Paper Fibre

## 4. THE FIBRE/FIBRE BOND FAILURE DAMAGE MECHANISM

The fibre structure shown in Figure 3(a) is the simplest structure that is able to simulate a fibre/fibre bond failure. The structure is essentially two fibres, perpendicular to one another, overlapping in the middle. A fibre/fibre bond exists where this overlap occurs, ‘gluing’ the two fibres together. To model the stresses present in the fibre structure, the horizontal fibre is stretched in the positive  $x$ -direction. The increased tension in the horizontal fibre causes the vertical fibre to bend. If the stress in the fibre/fibre bond is too great, the fibre/fibre bond will fail, allowing the vertical fibre to move freely. The failure process and resulting motion can be seen in Figures 3(b-d).

Therefore, the motion of the fibre structure after failure is similar to that of a plucked string. The frequency produced by a vibrating string is dependent on the tension ( $T$ ) within the string and the linear density ( $\mu$ ) of the string as stated by Rossing [12]. In terms of the mass/spring model it leads to the following relationship:

$$F_n = \frac{2n + 1}{2L} \sqrt{\frac{T}{\mu}} \quad \text{where: } T = kx, \mu = \frac{m}{L}, k = \frac{Etw}{L}, n = 0, 1, 2, \dots \quad (4)$$

In terms of the fundamental properties of a fibre, Equation (4) becomes:

$$F_n = \frac{2n + 1}{2L} \sqrt{\frac{Etwx}{m}} \quad \text{where: } n = 0, 1, 2, \dots \quad (5)$$

where  $E$  is the Young's Modulus,  $t$  is the thickness,  $w$  is the width,  $L$  is the free vibrating length and  $m$  is the mass of the paper fibre,  $x$  is the displacement of the paper fibre from equilibrium and  $n$  is the harmonic index. Using Equation (5) it is possible to predict how the changes in the fibre structure, due to the fibre/fibre bond failure damage mechanism, affect the frequency of vibration.

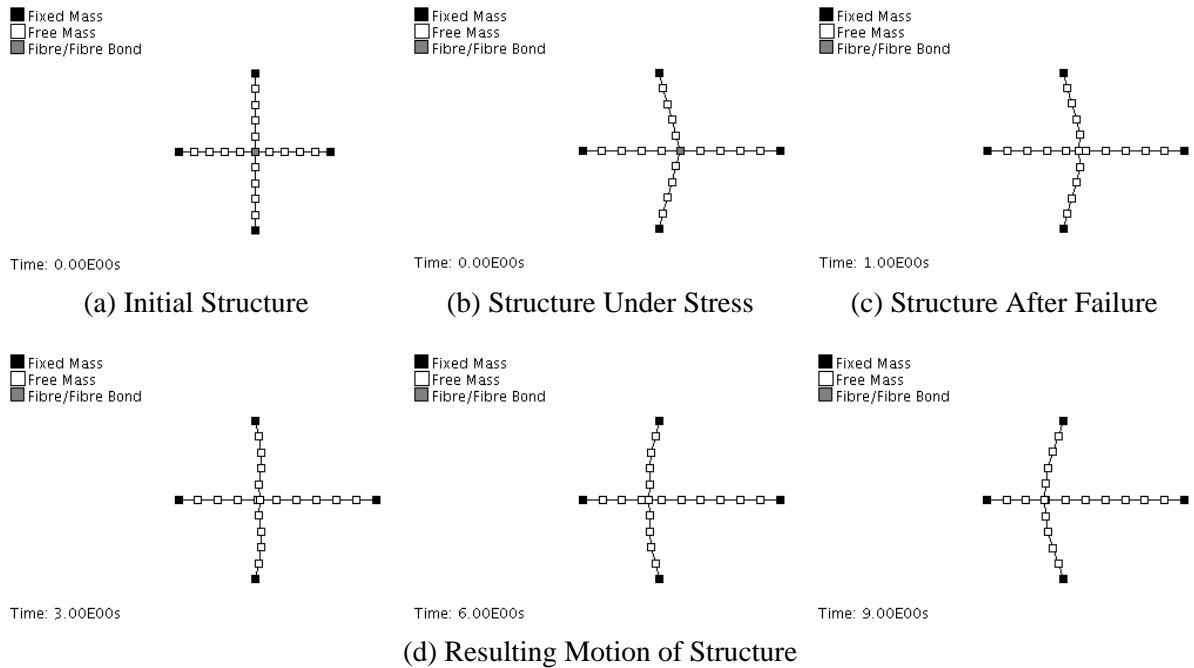


Figure 3 – The Fibre/Fibre Bond Failure Damage Mechanism

In terms of the fibre structure of paper, a mesh as shown in Figure 4, is a more realistic system for simulating a fibre/fibre bond failure as shown below.

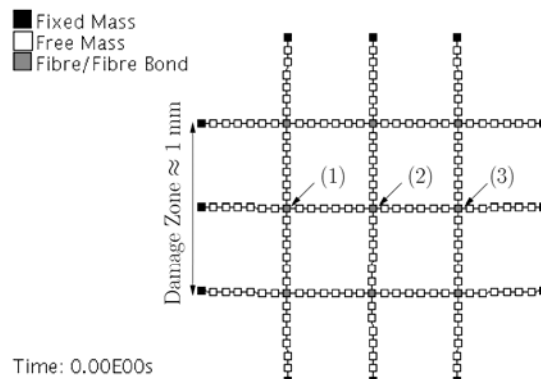


Figure 4 – 3x3 Cartesian Mesh showing Potential Fibre/Fibre Bond Failures

With reference to the setup of Figure 4, Figure 5 shows the CWT of the AE generated when fibre/fibre bond (1) fails, with Figure 6 showing the CWT from a typical experimental fibre/fibre bond failure. The experimental results are obtained from a tensile test for a notched paper specimen as stated by Graham *et al.* [13]. It is clear from the theoretical and experimental results that the fibre/fibre bond failure has two dominant frequency components at approximately 250 kHz and 750 kHz, which agrees with fundamental frequency and first harmonic of a paper fibre as defined by Equation (5), when using the material properties stated by Gregerson [11].

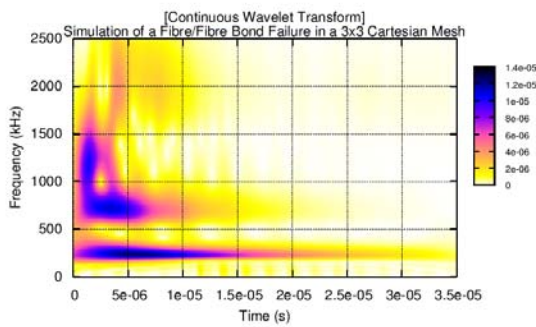


Figure 5 – Theoretical Fibre/Fibre Bond Failure

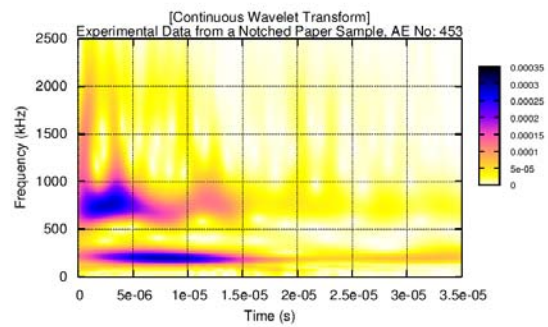


Figure 6 – Experimental Fibre/Fibre Bond Failure

## 5. THE FIBRE FAILURE DAMAGE MECHANISM

Returning to the second mechanism, the fibre structure shown in Figure 7(a) is the simplest structure that is able to simulate a fibre failure. The structure consists of a single fibre under tension. As the tension becomes too great, the fibre fails at some point along its length. At the point of failure, the fibre is no longer fixed at both ends, but consists of two smaller fibres, each with one fixed end. The failure process can be seen in Figures 7(b-d).

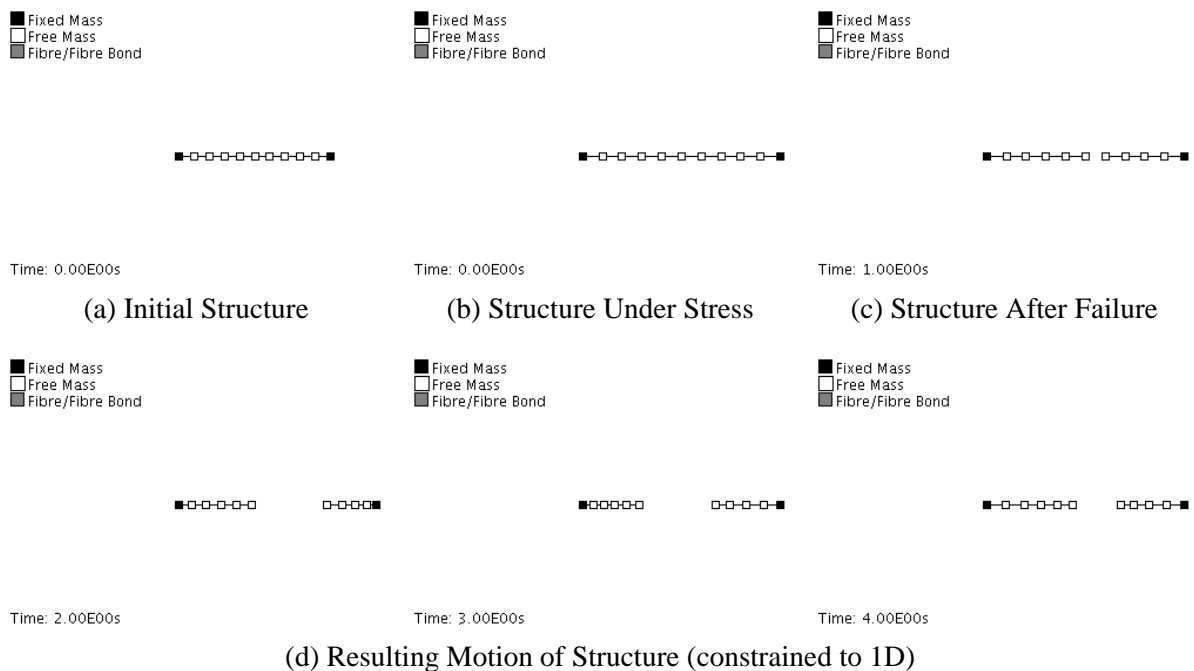


Figure 7 – The Fibre Failure Damage Mechanism

The motion of the two fibre halves after failure is that of a series of masses and springs in series. Consider a fibre that consists of a series of two masses and four springs with each end connected to a fixed point. The undamped equation of motion for the fixed fibre is defined as:

$$\begin{bmatrix} m_1 & 0 \\ 0 & m_2 \end{bmatrix} \begin{bmatrix} \ddot{x}_1 \\ \ddot{x}_2 \end{bmatrix} + \begin{bmatrix} 2k & -k \\ -k & k \end{bmatrix} \begin{bmatrix} x_1 \\ x_2 \end{bmatrix} = 0 \quad (6)$$

Where  $m_1$ ,  $m_2$ ,  $x_1$  and  $x_2$  are the masses and displacements on mass 1 and 2, respectively. Consider the same fibre, but in this case, only one mass is connected to a fixed point, with the other mass free to move. The undamped equation of motion for the free fibre is defined as:

$$\begin{bmatrix} m_1 & 0 \\ 0 & m_2 \end{bmatrix} \begin{bmatrix} \ddot{x}_1 \\ \ddot{x}_2 \end{bmatrix} + \begin{bmatrix} 2k & -k \\ -k & 0 \end{bmatrix} \begin{bmatrix} x_1 \\ x_2 \end{bmatrix} = 0 \quad (7)$$

A frequency analysis of Equations (6) and (7) produces the following natural frequencies of interest:

$$F_{\text{fixed}} = \frac{1}{2\pi} \sqrt{\frac{(3 \pm \sqrt{5})k}{2m}} \quad \text{and} \quad F_{\text{free}} = \frac{1}{2\pi} \sqrt{\frac{(2 \pm \sqrt{8})k}{2m}} \quad (8)$$

In terms of the fundamental properties of a fibre, Equation (8) becomes:

$$F_{\text{fixed}} = \frac{1}{2\pi} \sqrt{\frac{(3 \pm \sqrt{5})Etw}{2Lm}} \quad \text{and} \quad F_{\text{free}} = \frac{1}{2\pi} \sqrt{\frac{(2 \pm \sqrt{8})Etw}{2Lm}} \quad (9)$$

Using Equation (9) it is possible to predict how the changes in the fibre structure, due to the fibre failure damage mechanism, affect the frequency of vibration. When failure occurs, a long fibre section will vibrate at a frequency close to  $F_{\text{fixed}}$  and a short fibre section will vibrate at a frequency close to  $F_{\text{free}}$ . In terms of the fibre structure of paper, a mesh as shown in Figure 8, is more realistic system for simulating a fibre/fibre bond failure.

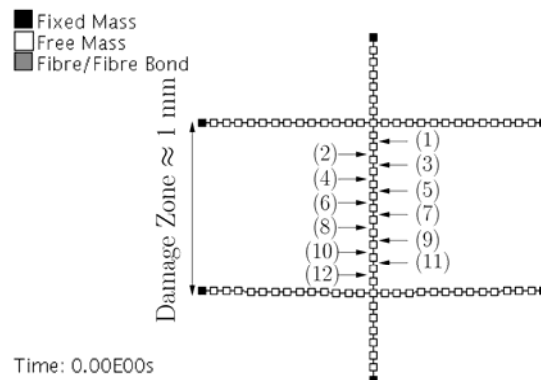


Figure 8 – 2x1 Fibre Structure showing Potential Fibre Failure Points

Figure 9 shows the CWT of the AE generated when the vertical fibre under tension, fails at point (7), with Figure 10 showing the CWT of a typical experimental fibre failure. It

is clear from the theoretical and experimental results that a fibre failure has a strong, but fleeting high frequency component at the beginning of the signal.

It is also interesting to look at the acoustic pressure contour plot resulting from the fibre/fibre bond failure and fibre failure damage mechanisms. Figure 11 shows that the acoustic wave generated from a fibre/fibre bond failure is similar to a dipole source and Figure 12 shows the acoustic wave generated from a fibre failure is similar to a linear quadrupole source.

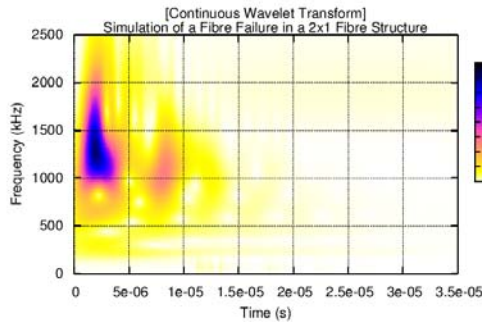


Figure 9 – Theoretical Fibre Failure

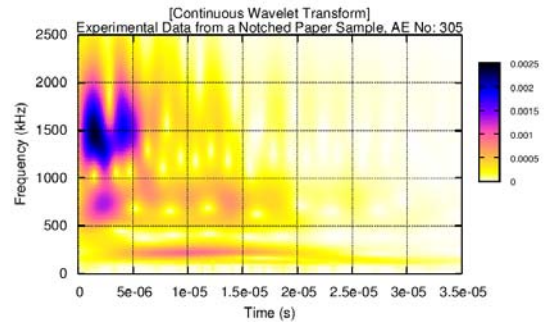


Figure 10 – Experimental Fibre Failure

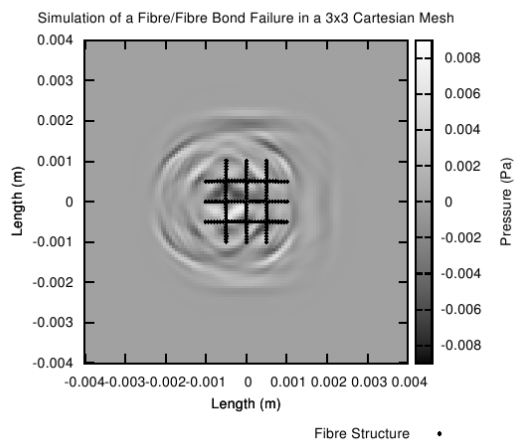


Figure 11 – Acoustic Pressure Contour Plot of a Theoretical Fibre/Fibre Bond Failure

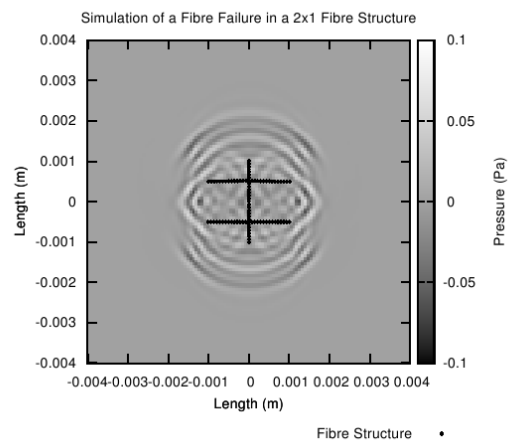


Figure 12 – Acoustic Pressure Contour Plot of a Theoretical Fibre Failure

From Figures 5 and 9 it is possible to define criteria from the CWTs for identifying the two damage mechanisms. The criteria for a fibre/fibre bond failure are listed below:

- The dominant frequency components of the AE must be at approximately 250 kHz or 750 kHz.
- The strongest frequency component may be at either approximately 250 kHz or 750 kHz.
- The duration of the frequency component at approximately 250 kHz is longer than that of the frequency component at approximately 750 kHz.

Finally, the criteria for identifying a fibre failure are given below:

- The dominant frequency component of the AE must be greater than 800 kHz
- The duration of the dominant frequency component must be less than 5.00E-06 seconds.
- The dominant frequency component must be present at the front of the AE.

## 6. CONCLUSIONS

This work has used a hybrid vibro-acoustic model that is able to provide an understanding of the micro-mechanics of the paper structure through the use of AEs by simulating the movement of simplistic fibre structures. The model is not limited to simple structures and can be used to reproduce an actual fibre mesh by copying a micrograph of paper or by generating a random mesh.

The fibre/fibre bond failure and fibre failure damage mechanisms are successfully modelled, with the results showing that differences exist between the two damage mechanisms, firstly in the physical properties of the fibre structure local to the point of failure and in the theoretical time/frequency representation of the resulting AE.

The differences in the behaviour of the local fibre structure are shown to be due to different mechanical analogues; the fibre/fibre bond failure damage mechanism is associated to a local fibre structure resembling a plucked string, whilst the fibre failure damage mechanism, relates to a local fibre structure that is similar to a series of vibrating masses and springs.

The differences in the CWTs of the two damage mechanisms show that the fibre/fibre bond failure results in a low frequency wave generated from a dipole source and the fibre failure results in a high frequency pulse generated from a linear quadrupole source. The time and frequency values as specified by the above criteria are dependent on the material properties of the paper fibres, as shown by Equation 4, but the shape of the CWTs is intrinsic to the physics of the damage mechanisms and should be present in any paper type. This result enables the dynamic identification of AEs during an experimental test and with further research can provide a gauge for the onset of fracture for a range of paper types. The paper used in this experiment is made from hand beaten chemical pulp (Nyström [14]).

## REFERENCES

- [1] D.Kao, *The vibro-acoustic modelling and analysis of damage mechanisms in paper*, PhD Thesis, The University of Greenwich, 2006.
- [2] D.Kao, K. Pericleous, D. Graham, B. Knight, "Use of a coupled mechanical-acoustic computational model to identify failure mechanisms in paper production", *Proceedings of the Thirteenth International Congress on Sound and Vibration (ICSV13)*, 2 - 6 July 2006, Vienna, Austria.
- [3] D. Baraff, A. Witkin, "Large steps in cloth simulation", *In Computer Graphics*, 43-45, SIGGRAPH (1998).
- [4] K-J. Choi, H-S. Ko, "Stable but responsive cloth", *In ACM Transactions on Graphics*, 604-611, SIGGRAPH (2002).
- [5] F. J. Fahy, *Sound Intensity*. (E & F N Spon, 1995).
- [6] A. Zakaria, J. Penrose, F. Thomas, X. Wang, "The two dimensional numerical modelling of acoustic wave propagation in shallow water", *Acoustics* (2000).
- [7] C. K. Chui, *An Introduction to Wavelets*. (Academic Press, 1992).
- [8] G. Kaiser, *A Friendly Guide to Wavelets*. (Birkhäuser, 1994).
- [9] R. K. Young, *Wavelet Theory and its Applications*. (Kluwer Academic, 1993).
- [10] H. Vallen, J. Vallen, "Free-of-cost software tools generate dispersion curves, perform wavelet transform and help correlate both kinds of information", Technical Report, Vallen-Systeme.
- [11] Ø. Gregerson, "Material properties of paper", Personal Communication, 2005.
- [12] T. D. Rossing, N. H. Fletcher, *Principles of Sound and Vibration*. (Springer-Verlag, 1995).
- [13] D. Graham, D. Kao, B. Knight, P. Gradin, P. Isaksson, S. Nyström, "Acoustic emission applied to mechanically loaded paper", *In 26<sup>th</sup> Conference on Acoustic Emission Testing, EWGAE* (2004).
- [14] S. Nyström, "Tensile paper test with a two sensor array", Experimental Data 2005-02-01, AEP QLK5-CT-2002-00772.